

RESEARCH

Open Access



Risk Assessment of Aged Concrete Gravity Dam Subjected to Material Deterioration Under Seismic Excitation

Tahmina Tasnim Nahar¹, Anh-Tuan Cao¹ and Dookie Kim^{2*}

Abstract

This paper proposes an approach to assess and predict the seismic risk of existing concrete gravity dams (CGDs) considering the ageing effect. The combination of fragility function and cumulative absolute velocity (CAV) depending on two failure states has been used in the analysis. It represents the time-variant degradation of the concrete structure and the conditional change of structural vulnerability in the case of the seismic excitation. Therefore, the seismic risk assessment captures here the nonlinear dynamic behavior of a concrete gravity dam through the fragility analysis. Incremental dynamic analysis for the fragility curves is adopted to state the performance of the dam in terms of different intensity measures. To assess the capacity of the aged concrete gravity dam, this research introduces a way to estimate the CAV_{limit} of CGDs with varying time. For a case study, an existing concrete gravity dam in Korea has been taken into consideration to apply this approach. The numerical finite element model is validated by optimizing the recorded field data. The proposed approach and its findings will be helpful to CGDs operators to ensure whether a dam needs to stop after a specific time using the extracted mathematical model. Furthermore, as this mathematical model is the function of time, the operator can get an idea about dam conditions at any specific time and can take necessary steps.

Keywords: capacity evaluation, seismic behavior, time-variant degradation, tensile cracking, relative displacement, fragility function, cumulative absolute velocity, capacity model

1 Introduction

The concrete gravity dams are the massive structure, and play an important role in multiple aspects, like flood control, power generation, agricultural work, water resource conservation, etc. It can create a hazardous condition to the surrounding environment and community if any failure happens after an earthquake (Hartford and Baecher 2004). For that reason, an enormous amount of research has been done until now about the structural health monitoring after an earthquake, seismic vulnerability

evaluation of existing dam and so on (Ansari and Agarwal 2016; Ansari et al. 2018; Fenves and Chopra 1986; Pan et al. 2009; Sen 2018; Tekie and Ellingwood 2003). The challenging issue is the ageing effect on a concrete gravity dam (CGD), where most of them are constructed for generally more than 50 years of design life (KCSC 2016) (depends on the purpose).

As CGD is impounded in the reservoir, one of the reasons to have damage induced due to the moisture and heat transport, freeze–thaw actions, chemically expansive reactions, and chlorides of reinforcing steel with time (Bangert et al. 2003; Champiri et al. 2018; Kuhl et al. 2004a; Wan et al. 2012). These reasons may cause the extension of micro-cracks and the opening in the cementitious skeleton, which affects the durability of the concrete structures by reducing the concrete strength

*Correspondence: kim2kie@kongju.ac.kr

² Department of Civil & Environmental Engineering, Kongju National University, 1223-24 Cheonan-daero, Seobuk-gu, Cheonan, Chungcheongnam-do 31080, Republic of Korea
Full list of author information is available at the end of the article
Journal information: ISSN 1976-0485 / eISSN 2234-1315

(Bangert et al. 2001; Ghrib and Tinawi 1995; Gogoi and Maity 2007; Kuhl et al. 2004b). According to Nakamura et al. (2018), the experimental result showed that the crack propagation on concrete will reduce the compressive strength and compressive fracture energy. The CGDs bounded by the water bodies are subjected to these effects and are named by the chemo-mechanical model, which is used in this study for assessing and predicting the seismic risk of CGDs. The chemo-mechanical effect has been used in the previous study (Gogoi and Maity 2007; Nayak and Maity 2013; Wang et al. 2011) for especially CGD in case of seismic performance. Most of that research was related to the structural response in case of stiffness, stress and displacement.

Very few researches have been done (Dong et al. 2013; Ghosh and Padgett 2010) on the seismic vulnerability assessment of the time-dependent fragility curve. The analysis of these researches focuses on other structural seismic performance except the CGDs. Nevertheless, this study introduces a correlation between the chemo-mechanical effect on CGDs and the seismic performance of the structure with time. To do this, the fragility function is acted here as a key component for the seismic loss assessment. Fragility curves describe the probability of failure, which is the best way to estimate and determine the vulnerability of the potential damage of the structure in the future (Ansari and Agarwal 2016). The uncertainty analysis for the fragility function is estimated by determining the High Confidence Low Probability of Failure (HCLPF) of the structural response (Kim et al. 2011).

Incremental dynamic analysis (IDA) described by Baker (2015) is used in this study to draw the fragility curve based on two limit states (presented in this paper as LS1 and LS2) (Sen 2018; Tekie and Ellingwood 2003). The 30 selected earthquakes provided by K-water organizations are taken for applying the proposed methodology to the Bohyeonsan concrete gravity dam in Korea. Different intensity measure (IM) (Mazilgüney et al. 2013) is carried out to demonstrate the fragility function. To show the threshold value of quantifying the seismic risk of structure, the peak ground acceleration (PGA), spectral acceleration (Sa), and cumulative absolute velocity (CAV) have been adopted. In 1988, the Electric Power Research Institute (EPRI) introduced cumulative absolute velocity (CAV) as a potential damage-related ground motion IM (Campbell and Bozorgnia 2012). Most of the previous study on CAV was related to Nuclear Power Plants (NPP) (Hardy et al. 2006). However, the proposed approach has inaugurated a way to estimate CAV for seeing the capacity value of CAV_{limit} for aged CGDs. The CAV has higher predictability than other IMs such as the PGA (Du and Wang 2013) for giving the safety measurement by predicting the capacity of the structure. According to Heo

and Kunnath (2013), the seismic response has been evaluated by damage-based performance.

Therefore, this research proposes an approach for assessing and predicting the seismic capacity evaluation of CGDs accounting with the chemo-mechanical effect. With the combination of fragility function and CAV, finally, it provides a capacity model using which the investigators or engineers can get the capacity limit for the aged CGDs through the threshold value of PGA at any time. Generally, the CGDs are practically experienced by different environmental and surrounding conditional effect, where this capacity model will give the CGDs strength at that practical condition. Besides predicting and assessing the seismic risk of CGDs with time, this approach also gives a process of how to consider the surrounding practical effect (here chemo-mechanical effect). This process has been carried out here for the Korean earthquake and the approach also can be updated for any regional earthquake.

2 Theoretical Background

In the previous study, a time-dependent isotropic damage index based on the chemo-mechanical effect of concrete material was shown by the loss of stiffness along with its height, displacement and stresses (Gogoi and Maity 2007; Nayak and Maity 2013; Wang et al. 2011). This study has proposed a methodology to evaluate the safety measurement by the effect of chemo-mechanical on concrete material through the combination of fragility analysis and CAV. For implementing this methodology, the numerical analysis has been done and for optimization, the numerical model validation and verification are needed. Therefore, this section will introduce the step-by-step related theoretical background of the proposed approach.

2.1 Numerical Model Optimization by Validation and Verification

For validating the numerical model, the response surface methodology (RSM) according to Myers et al. (1995), analyzes the relationship between several variables (u) and responses (m) of the structure by the following mathematical model:

$$m = f(u_1, u_2, \dots, u_k) + v, \quad (1)$$

where v describes the error observed in the response m and $f(u_1, u_2, \dots, u_k)$ transmits the response of the structure due to the sets of input variables. In RSM generally, a first-order and second-order polynomial equations are used. Usually, the second order is sufficient to solve the engineering problems and in this study, which is presented as following Eq. (2):

$$m = \eta_0 + \sum_{i=1}^k \eta_i u_i + \sum_{i=1}^k \eta_i u_i^2 + \sum_{i,j=1}^k \eta_{ij} u_i u_j + \nu, \quad (2)$$

here m is the response of prediction and η is the estimated partial regression coefficient; u_i is the coded factor ($i, j = 1, 2, 3 \dots, k$) and ν is the offset term. The polynomial equation can be used in higher order.

A design experiment tool called central composite design (CCD) (Sadhukhan et al. 2016) is used to predict the output using the equation based on central and axial points with a factorial design for optimization of the response of the structure. Using the Eq. (3), the total experimental number can be created using the CCD tool.

$$N = 2^k + 2k + c_q, \quad (3)$$

here, k is the number of factors and c_q the number of center-point. For accurately amplifying the CCD method in this study, two parameters are used such as the coefficient of Young's modulus and density.

After identifying the system of the numerical model, it is an essential factor to verify the model with previous studies. The fundamental frequency of the model will be compared with Eq. (4) according to Fenves and Chopra (1986).

$$T_{\text{ref}} = 1.4 \frac{H}{\sqrt{E}}, \quad (4)$$

where H is the height of the concrete gravity dam. Besides that, the check for the crest spectral acceleration (g) is also a verification factor along with the modal shape. Also, the frequency domain decomposition (FDD) method has been adopted to verify the fundamental frequencies, which is explained more detailed in Sect. 3.4.

2.2 Chemo-mechanical Model for Aged CGD

From the experimental results, Washa et al. (1989) developed the governing equation for considering the time effects on the compressive strength of a concrete gravity dam, which can be exhibited by Eq. (5).

$$f_c(t_a) = 3.75 \ln(t_a) + 44.33, \quad (5)$$

where t_a is the age of concrete in years, and $f(t_a)$ is the compressive strength gained after time. Taking into account the gain in compressive strength of the sound concrete with age (Washa et al. 1989), the value of static elastic modulus in SI is obtained from the following expression (Mandal and Maity 2015):

$$E_0 = 4733 \sqrt{f(t_a)}. \quad (6)$$

However, for the external loading and surrounding environmental effects, the concrete material is damaged,

and these damages will increase with the time (Kuhl et al. 2004b). This damage is manifested as the porosity of concrete and Eq. (7) shows the total porosity of concrete.

$$\phi = \phi_0 + \phi_c + \phi_m, \quad (7)$$

here, ϕ is the total porosity, ϕ_0 is the initial porosity, ϕ_c is chemical porosity, and ϕ_m is the apparent mechanical porosity. The mechanical porosity ϕ_m is defined by the Eq. (8).

$$\phi_m = [1 - \phi_0 - \phi_c] d_e, \quad (8)$$

where d_e is the scalar degradation parameter and the function of this parameter has been expressed (Gogoi and Maity 2007; Mandal and Maity 2015; Nayak and Maity 2013) as the following equation:

$$d_e = \alpha_s - \frac{k_m^0}{k_m} \left[1 - \alpha_m + \alpha_m \exp\left(\beta_m [k_m^0 - k_m]\right) \right]_m, \quad (9)$$

here, k_m^0 and k_m are the values of strain that represent the initial damage and is the maximum value of strain during loading history, respectively. If there is no degradation due to mechanical loading, the k_m may be considered as k_m^0 ; as a result of the d_e and ϕ_m is zero and α_m, β_m are parameters that have been taken here from Bangert et al. (2003). The value of α_s will differs from 1 to 0 because of the degradation and non-degradation, respectively.

The relation between non-degraded Young's modulus of elasticity E_0 and degraded Young's modulus of elasticity by the porosity effect of the concrete is $E_e = (1 - d_e)E_0$ (Mandal and Maity 2015; Nayak and Maity 2013). Therefore, from Gogoi and Maity (2007), the time-varying damaged modulus of elasticity of concrete can be written by the following equation:

$$E_e = (1 - \phi)^{\frac{t_a}{T_a}} E_0. \quad (10)$$

2.3 Seismic Risk Assessment of Aged CGD

2.3.1 Fragility Function

Several studies are available regarding the failure criteria under the post-earthquake conditions for every structure. The main failure mechanisms generally are investigated as the drift deformation of the dam body, cracking at the dam neck, and material failure on compression or tension. These failures occur either in the foundation, in concrete at the toe or the dam-soil interface, etc. (Tekie and Ellingwood 2003). According to the observation (Lupoi and Callari 2011), the failure behavior of the CGD can be categorized based on some particular zone. Among those specific zones, (i) the dam-foundation interface region, (ii) the main body of the dam and (iii) above the neck region is main. From these three categorized zones, (i) and (ii) are

the more general case. In this study, to take consideration of the general case, two limit states have been considered from the general failure pattern. Tensile damage state is termed as LS1 (Tekie and Ellingwood 2003) (measured from a split cylinder test) is described by Mirza et al. (1979).

$$f_{sp} = 6.4\sqrt{f_{c'}}, \tag{11}$$

where f_{sp} = splitting strength of concrete (psi).

And the other one is the relative crest displacement which with respect to the dam heel is considered as LS2. The value of LS2 is calculated as 0.028% of dam height is taken from Sen (2018) and Tekie and Ellingwood (2003).

The method to develop the fragility function in this study is the classical lognormal approach including maximum likelihood estimation (MLE) (Baker 2015; Mandal et al. 2016), which can be written by the following equation:

$$P(C|IM) = \varphi \left[\frac{\ln \left(\frac{IM}{\theta} \right)}{\beta} \right], \tag{12}$$

where P is the probability that a GM with $IM = x$ induces the collapse of a structure, $\varphi()$ is the standard normal cumulative distribution function, θ is the median of the fragility function and β is the standard deviation of $\ln IM$ (Baker 2015). Making the reasonable assumption that the IM_i value for each GM is independent, the likelihood of the entire data is observed as follows:

$$\text{likelihood} = \prod_{i=1}^m [P(C|IM)]^{p_i} [1 - P(C|IM)]^{q_i}, \tag{13}$$

where m is the number of IM levels, Π is the product overall levels, $p = 1$ or 0 depending on whether or not the cases exceed the Limit State (LS) and $q = 1 - p$.

The most common method to explain the fragility is incremental dynamic analysis (IDA), which involves a series of structural dynamic analyses under a set of ground motion records. This set of recorded data is scaled to several intensity levels. According to Ibarra and Krawinkler (2005), the fragility curve is calculated from data sets by taking logarithms of each ground motion's value corresponding to the onset of the collapse. The median and standard deviation of the fragility curves are shown by Eqs. (14) to (15):

$$\ln \theta = \frac{1}{n} \sum_{i=1}^n \ln IM_i, \tag{14}$$

$$\beta = \sqrt{\frac{1}{n-1} \sum_{i=1}^n (\ln(IM_i/\theta))^2}. \tag{15}$$

The marginal assessment of seismic evaluation focuses on the high confidence of low probability of failure (HCLPF). It is defined as the level of earthquake ground motion at which there is a 95% confidence of an at most 5% probability of failure (Prassinos et al. 1986). The HCLPF capacity can be obtained by a component that requires the estimation of its seismic response as a function of the seismic margin earthquake (SME) and its seismic capacity (Nie et al. 2010) as shown in Fig. 1. From the mean fragility curve C_{HCLPF} can be estimated by the following equation:

$$C_{HCLPF} = C_{1\%} = C_{50\%} e^{-2.326\beta_C}, \tag{16}$$

where β_C is the composite logarithmic standard deviation, which is the replacement of epistemic uncertainty and random variability.

2.3.2 Cumulative Absolute Velocity (CAV)

To ignore the unnecessary shutdowns of any structure after the earthquake, a new ground motion IM called CAV at first proposed by EPRI in the 1980s for safety measurement. CAV is defined as the integration of the absolute value of the acceleration time series (Campbell and Bozorgnia 2012; Wang et al. 2018) which is explained mathematically by Eq. (17):

$$CAV = \int_0^{t_{max}} |a(t)| dt, \tag{17}$$

where $a(t)$ is acceleration value, t is time, and t_{max} is the total duration of the time series. In some cases, only the acceleration whose peak value exceeds a threshold value of 0.025 g within a 1-s time interval has to be calculated termed as CAV_{STD} proposed by O'Hara and Jacobson (1991).

The CAV limit shows the capacity of the structure based on the HCLPF point from the fragility. Using the

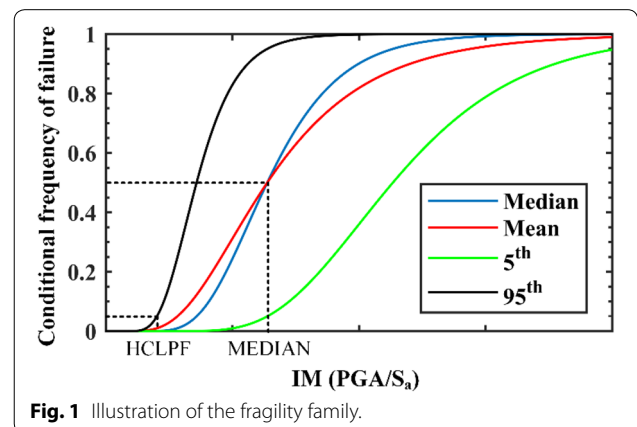


Fig. 1 Illustration of the fragility family.

IM in terms of peak ground acceleration from HCLPE, the ground motion data set are being scaled for getting the CAV values. The mean value from these CAV becomes the limit value of the capacity of the structure. Also, the 5% failure probability in fragility with respect to CAV (as IM) will give the structural capacity.

3 Case Study of the Proposed Approach

3.1 Description of Sample CGD

For assessing the seismic performance of a CGD with time-varying ageing effects, Bohyeonsan multipurpose CGD has been selected. This dam is located in the upper stream of Gohyeoncheon, which is the second tributary of the Kumho River in South Korea. Figure 2a presents the location of the sensors to get earthquake measurement data and Fig. 2b shows the sectional detailing. The dam belongs to the total crest length is 250 m and the maximum height is 57 m. This dam significantly is used for the controlling of reservoir water, the full storage capacity of the reservoir is $22.10 \times 10^6 \text{ m}^3$ and the construction of the dam was completed in 2014. The crest width of the dam is 11.15 m and the height varies from 34.5 to 57.0 m. Table 1 shows the specification of this dam.

3.2 Finite Element Model (FEM)

For seismic analysis of the Bohyeonsan dam, a two-dimensional finite element model is presented here by using ABAQUS. The FEM for the selected section (Fig. 2b) from the 3D view of the dam (Fig. 2a) is illustrated in Fig. 3. The sectional view is shown in Fig. 2b; it can be seen that this dam is built using two kinds of concrete with different elastic modulus. The dam material property was taken from Table 1 and the dimensions are shown in Fig. 3 as well as the mesh distribution. The mesh size in the model was assigned in such division that

Table 1 Detailing of Bohyeonsan dam.

Material properties	Inside the dam	Outside the dam
Compressive strength (MPa)	12	18
Young's modulus (MPa)	13,767	16,861
The tensile strength (MPa)	1.3	1.6
Poisson's ratio	0.18	0.18
Density (kg/m ³)	2300	2300

the number of finite elements for the concrete inside and outside material was 500 and 358, respectively. The FEM consists of 4 nodes, bi-linear, plane strain quadrilateral elements (CPE4R) (Fig. 3) considering reduced integration and hourglass control (Al-Shadeedi and Hamdi 2017).

The non-linear dynamic analysis was carried out by adopting the implicit integration method accounting with the gravity load due to its self-weight as a static condition and ground horizontal acceleration of selected earthquakes as the seismic condition. The upstream wall was subjected to the water pressure up to 42.82 m, where the interaction between dam and water is considered here as a dynamic effect resulting from the transverse component of ground motion. This was simply modeled as added mass at the interface of dam–water and calculated using the Westergaard (1933) formula, which is also used in several studies (Alembagheri and Ghaemian 2013; Ansari et al. 2018; Nguyen et al. 2019). According to the Westergaard (1933), in Fig. 3 to assign the water pressure, the added masses were taken at each node (25 nodes) at the interface of the dam and reservoir using the following equation:

$$m_i = \frac{7}{8} \rho_w \sqrt{h_w (h_w - y_i)} \frac{(L_{i+1} + L_i)}{2}. \tag{18}$$

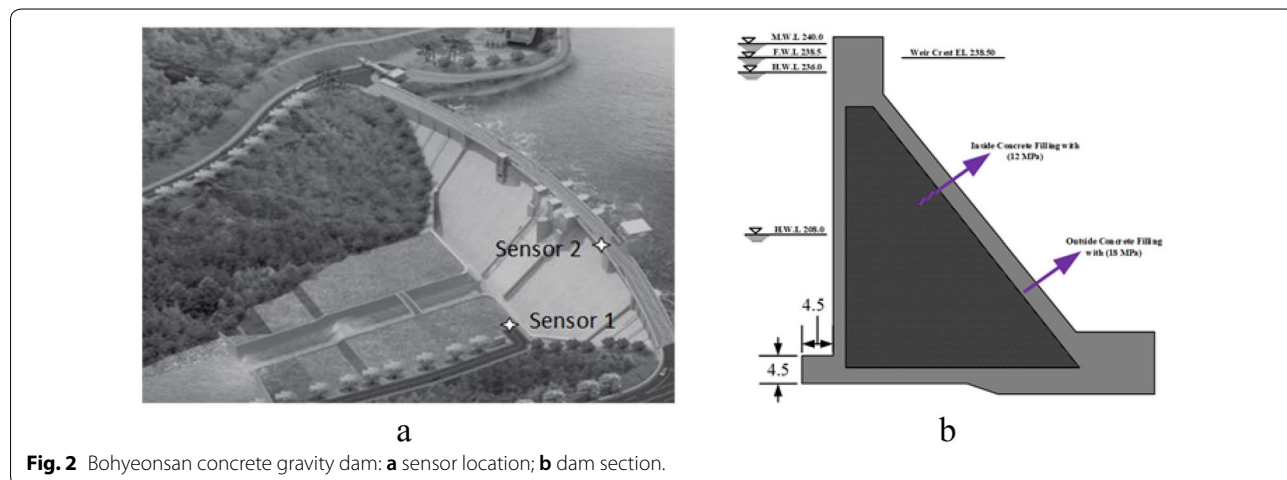


Fig. 2 Bohyeonsan concrete gravity dam: **a** sensor location; **b** dam section.

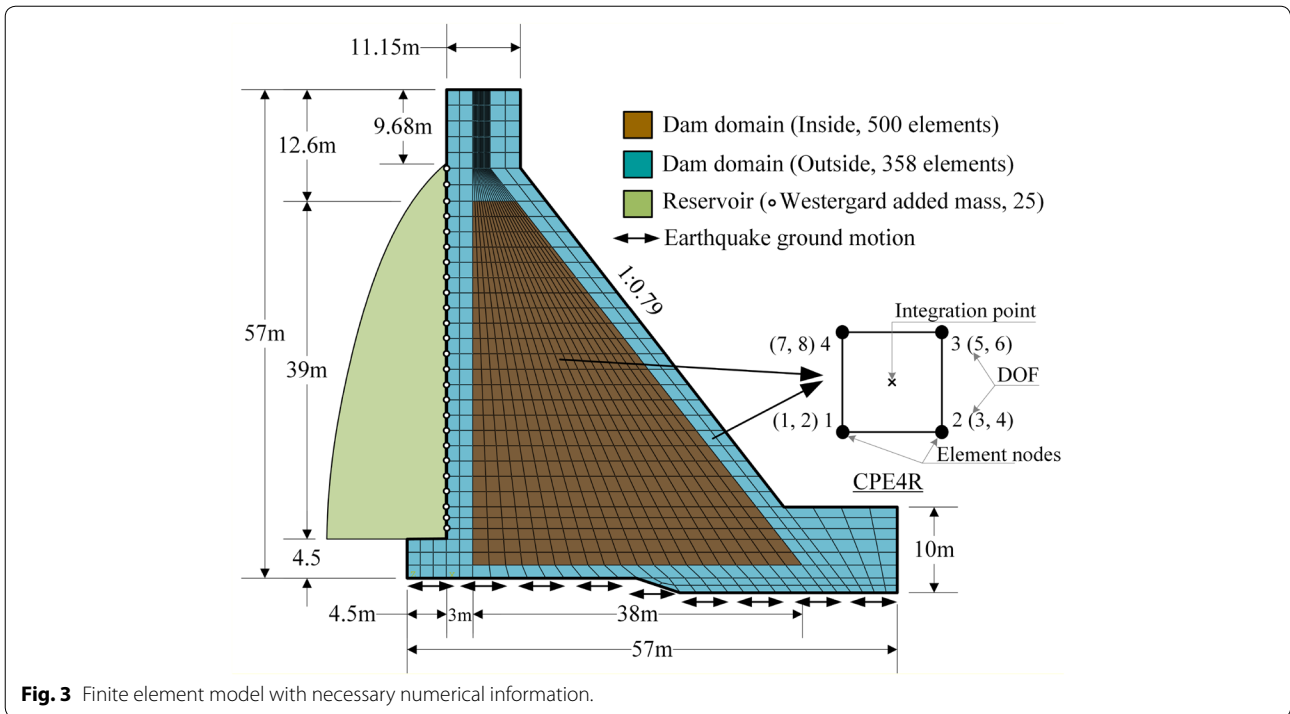


Fig. 3 Finite element model with necessary numerical information.

The vertical hydrodynamic components due to the ground motion were neglected in the simulations and the rigid foundation was used for bedrock condition. To consider the free-field motion during an earthquake, it was applied at the dam base as shown in Fig. 3. Here, only the horizontal ground motion data are considered for seismic analysis of the dam (Alembagheri and Ghaemian 2013). For the optimization of the model, which will be explained later, the free-field data of the Pohang earthquake were used as the input ground motion.

The damping matrix, according to the Rayleigh method (Chopra 2011), is adopted here, applied by Mridha and Maity (2014). Considering 5% damping ratio in both inside and outside concrete, the damping coefficients can be calculated by a linear combination of the stiffness matrix $[K]$ and the mass matrix $[M]$ as follows:

$$[C] = \alpha[M] + \beta[K], \tag{19}$$

where α and β are the mass-proportional and stiffness-proportional coefficients, respectively.

The following dynamic equation of motion can explain the above two-dimensional discretized FEM system.

$$[M]\{\ddot{u}\} + [C]\{\dot{u}\} + [K]\{u\} = [M]\{\ddot{u}_g\} + \{p\}, \tag{20}$$

where $[M]$, $[C]$ and $[K]$ are the mass, damping and stiffness matrix, respectively. $\{u\}$ is the displacements vector of the nodal point relative to the free-field ground displacement at the dam base, $\{\dot{u}\}$ and $\{\ddot{u}\}$ are the relative

velocity and acceleration vectors, respectively. $\{\ddot{u}_g\}$ is the free-field ground acceleration and $\{p\}$ is the total pre-seismic load associated with the gravity and hydrodynamic added mass.

This FEM system was taken all through the seismic analysis as well as structural system identification of this study.

3.3 Material Model for Concrete

For non-linear analysis of the material model, the concrete damage plasticity model (CDP) was considered. This model can be expressed as the complete inelastic potential behavior, which also can develop proper damage simulation for concrete both in tension and compression. In addition, this model can analyze the concrete structure under the loading combinations both static and dynamic and, thus, enable the transfer of results between the two (Wahalathantri et al. 2011). In the CDP model, the post-failure behavior under compression is defined by a softening stress–strain response and tension stiffening is specified either by means of post-failure stress–strain behavior in tension or by applying a fracture energy cracking criterion.

The CDP model describes that the concrete has significant volume change, when subjected to severe inelastic stress states, commonly referred to as dilation. In this study, the dilation angle has been taken as 36°, while default values were assumed for all other plasticity parameters.

The origin of the non-linearity can be introduced to various system properties such as materials, geometry, non-linear loading, and constraints. To meet the non-linear property, some material parameters are induced as the input data in Table 2.

According to the EN1992-1-1, stress–strain behavior of plain concrete in uniaxial compression is defined as the typical stress–strain relationship for nonlinear structural analysis of concrete. For introducing this the equations are followed by this for concrete compression behavior from EN1992-1-1, where the relationship between the compressive stress, σ_c and shortening strain, ε_c for short-term uniaxial loading is described by the following equation:

$$\frac{\sigma_c}{f_{cm}} = \frac{k\eta - \eta^2}{1 + (k - 2)\eta}, \tag{21}$$

where σ_c is the compression stress in concrete, $\eta = \frac{\varepsilon_c}{\varepsilon_{c1}}$, ε_c is the compressive strain in the concrete, ε_{c1} is the compressive strain in the concrete at the peak stress f_c and $k = \frac{1.05E_{cm}|\varepsilon_{c1}|}{f_{cm}}$. Figure 4a shows the uniaxial compression stress–strain behavior of the outside concrete material of the Bohyeonsan dam for each year (0, 10, 20, 30, 40 and 50 years) because the outer material is more vulnerable.

Table 2 Default parameters for the CDP model (Birtel and Mark 2006).

Parameters	Dilatation angle	Eccentricity	f_{bo}/f_{co}	κ
Value	36°	0.1	1.16	0.667

In the case of a tension stiffening approach for concrete exponential tension softening model was used (Cornelissen et al. 1986). This is one of the ways of concrete softening response using a fracture energy concept. Therefore, the post-failure tensile behavior is defined using the following exponential function:

$$\frac{\sigma_t}{f_t} = f(w) - \frac{w}{w_c}f(w_c), \tag{22}$$

$$f(w) = \left[1 + \left(\frac{c_1 w}{w_c} \right)^3 \right] \exp \left(- \frac{c_2 w}{w_c} \right), \tag{23}$$

where w is the crack opening displacement, w_c is the crack opening displacement at which stress can no longer be transferred, c_1 and c_2 are material constants for normal concrete. Figure 4b shows the material softening behavior in tension for each year similarly as the behavior in compression and the maximum σ_t follows the splitting strength of concrete using the Eq. (11). As the cracking was started just after this tensile stress, these values were taken for the tensile damage limit states in seismic fragility analysis. From Fig. 4, it is clarified that the damage input parameters showed the effect of fracture behavior along with the effect of degradable material property. Chemo-mechanical model changes the modulus of elasticity with time and produced micro-crack propagation, which causes the tensile crack in the CGD body. As we saw the fracture behavior of the concrete in Fig. 4, it indicates how much crack displacement will dominate the concrete strength as well as the concrete durability. For the seismic capacity evaluation, the concrete tensile damage is taken for showing the failure probability with damage consideration.

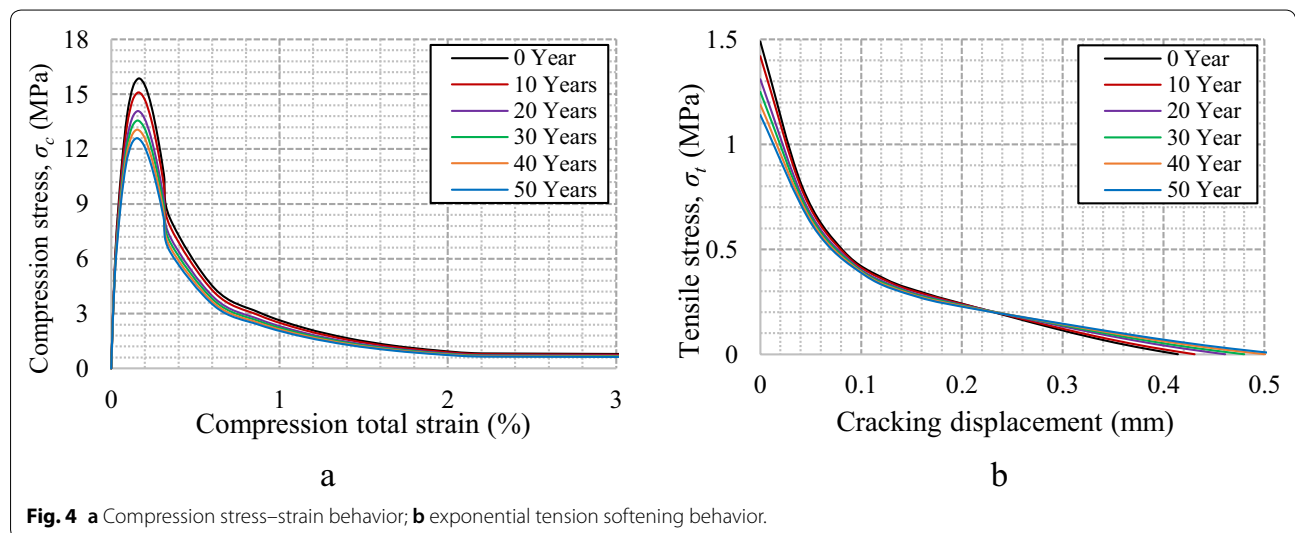


Fig. 4 a Compression stress–strain behavior; b exponential tension softening behavior.

3.4 Validation and Verification

As shown in Fig. 2b, the value of E for inside and outside of the dam is different. For decreasing the number of runs and to keep the same ratio of inside and outside parameters, the same coefficient of E (CoE) (i.e., a multiplying factor of E which will be used to get the original value of E) was taken for CCD. Therefore, the numerical model parameters are generated by considering two variables such as CoE and ρ , respectively. The acceleration on the top of the dam under Pohang-earthquake has been counted as a structural response. Pohang earthquake is one of the strongest recorded earthquakes in the Korean Peninsula with magnitude 5.5, which occurred on November 15, 2017 (Grigoli et al. 2018).

CCD has created a total of 9 points using the Eq. (3) and after optimization, the final value of CoE and density is 0.787 and 2.32 (tone/m³), respectively. However, the seismic analysis was then carried out using the optimized parameters enlisted in Table 3.

To understand the validation by RSM method, Fig. 5 shows the response spectrum at the top of the dam before and after optimizing. It is observed that the difference between the peak acceleration and frequency is decreased when compared with the recorded data. By analyzing Fig. 5 and Table 4, it is shown that the response of the dam after RSM is not exactly matched because of many uncertain factors. However, if we consider the

percentage of similarities, we can say that the results are acceptable.

After validation of the FEM, modal identification was verified here by comparing the fundamental frequencies with the previous study and existing method. The fundamental frequencies were observed from the optimized FEM simulation and the recorded data were extracted using frequency domain decomposition (FDD) methods. The FDD is a technique for the decomposition of the system response from recorded data to identify the fundamental parameters described in Brincker et al. (2000). This technique follows simple decomposition each of the estimated spectral density matrices. The singular values of the power spectral density (PSD) function matrix $S_{yy}(\omega)$ are used to estimate the natural frequencies instead of the PSD functions themselves as follows:

$$S_{yy}(\omega) = U(\omega)^T \sum (\omega) V(\omega), \tag{24}$$

where \sum is the diagonal matrix consisting of the singular values (σ_i 's) and U and V are unitary matrices. Since $S_{yy}(\omega)$ it is symmetric, U becomes equal to V (Ko et al. 2009).

From the FDD extraction, the fundamental frequencies were acquired analyzing the recorded data in Fig. 6. The analysis shows two peaks that were observed through the resonant frequencies and corresponding fundamental frequencies are listed up in Table 5.

Table 3 Material properties of the validated model.

Material properties	Inside the dam	Outside the dam
Modulus of elasticity, E (MPa)	10,835	13,269
Poisson ratio, μ	0.18	0.18
Density, ρ (tone/m ³)	2.32	2.32
Damping ratio, ξ (%)	5	

Table 4 Comparison of RS between before and after optimization.

	Before optimization	After optimization
Similar (%)		
Acceleration	92.8	97.3
Frequency	93.3	96.7

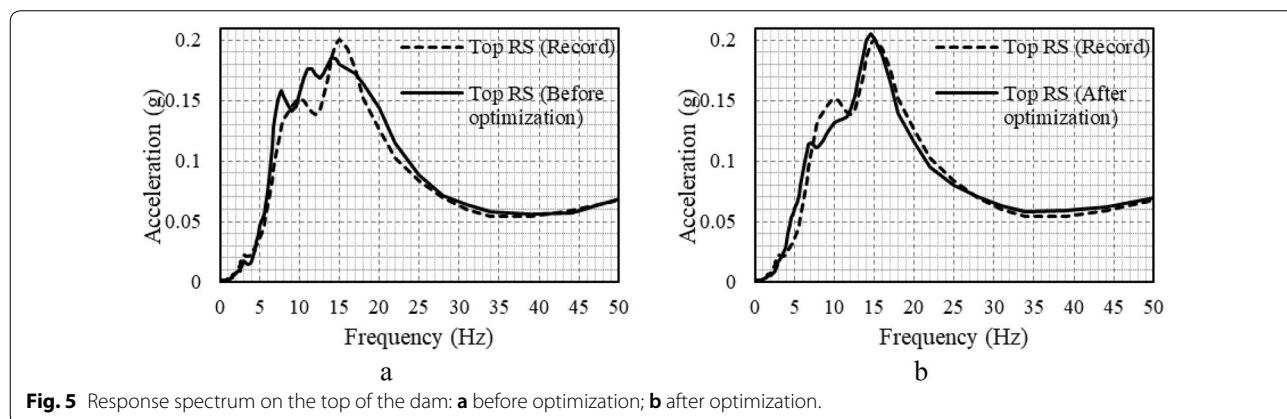


Fig. 5 Response spectrum on the top of the dam: **a** before optimization; **b** after optimization.

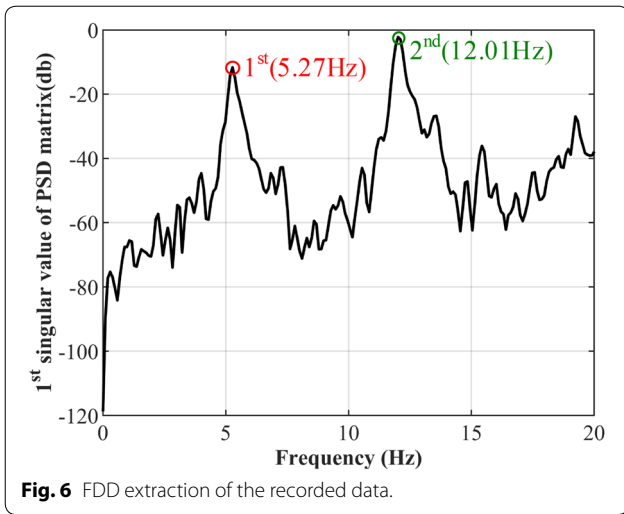


Fig. 6 FDD extraction of the recorded data.

Table 5 Comparison of fundamental frequencies.

Fundamental frequencies	References		This study FEM	CoV	
	(1) FDD (Ko et al. 2009)	(2) Eq. (4) (Fenves and Chopra 1986)		With (1)	With (2)
1 st	5.27	5.052	5.3467	0.01	0.04
2 nd	12.01	-	12.557	0.03	-

Alongside this, the 1st fundamental frequency of the optimized FEM (Fig. 7) is compared with Ref. 1 and Ref. 2 (Table 5). From Table 5, it is observed that for the first mode, the rate of accuracy is 1.4% with Ref. 1 and 5.83% with Ref. 2, respectively. Similarly, for the second mode, the result claims an accuracy of around 4.55% with Ref. 1. Inert to be acceptance of FEM result verification, acceptance value is less than 15% (Shah 2002), where this study shows the most approvable result. Also analyzing the CoV in the last column of Table 5, it can be said that the FEM result has a good agreement with the FDD result and also with the previous study (Eq. 4). The acceptable result for CoV was taken here for verification according to Pakzad (2018). Therefore, the FEM model is validated and verified now for further analysis.

3.5 Damaged E_e of Aged CGD

To determine the damaged modulus of elasticity (E_e), a degradation function d_e is calculated from Eq. (9). In this equation, material parameters are taken as $\alpha_m = 0.9$, $\beta_m = 1000$, $\phi_0 = 0.2$, and $k^0 = 0.00011$ to consider the deterioration effect of concrete material. The value of chemical porosity ϕ_c considered in this study is 0.2 (Gogoi and Maity 2007; Kuhl et al. 2004b). The reduction of the modulus of elasticity due to porosity with the varying time has been calculated, using Eq. (10), where the sound modulus of elasticity is calculated using Eq. (6). A graphical representation is shown in Fig. 8 using the

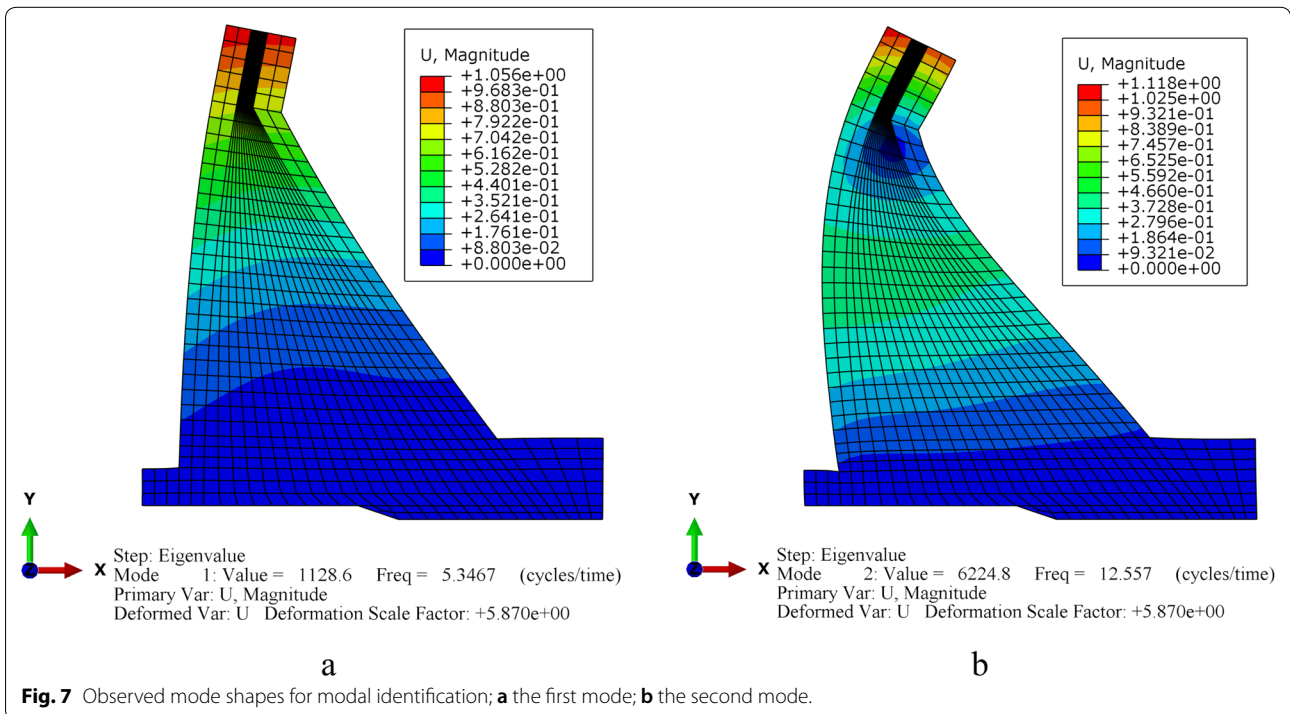


Fig. 7 Observed mode shapes for modal identification; a the first mode; b the second mode.

sound and damaged modulus of elasticity of the Bohyeonsan Dam. From Fig. 8, it is observed that the elastic modulus of sound concrete is increased with increasing time and after considering the chemo-mechanical damage, the elastic modulus is decreased with time.

3.6 Ground Motion Database

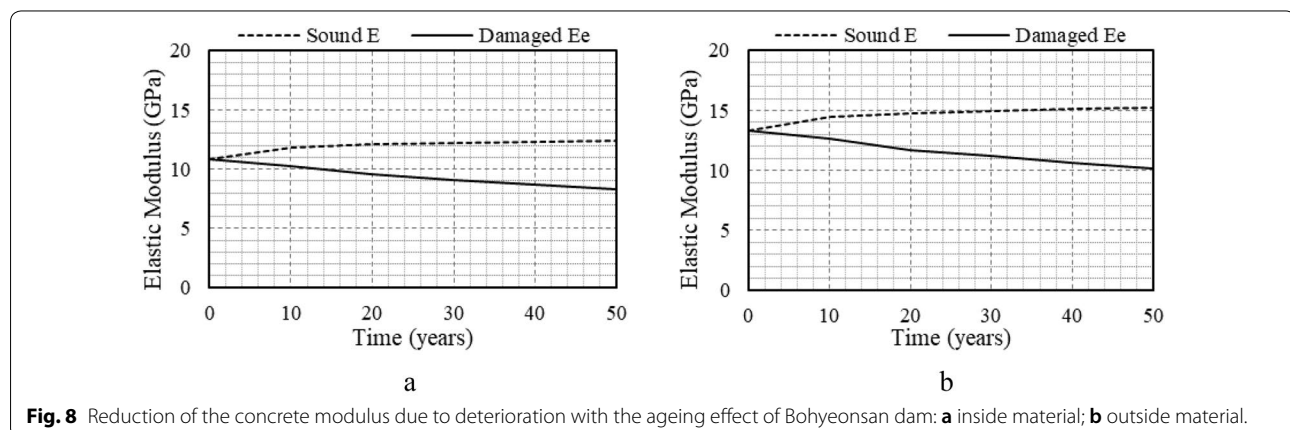
Ground motion randomness is carried out by taking 30 unscaled earthquake datasets from *k* water organization in Korea. Due to the presence of uncertainty in ground motion, the target spectrum is obtained from KDS 41 and soil class S1 (rock type soil) (KCSC 2019). The selection criteria are followed here according to the design spectra explained in Manandhar2b and Cho (2018). However, the vertical component is ignored here because of comparatively less acceleration than other components. The strongest horizontal component is taken here from the field data record based on the strong duration, i.e., 5–75% area intensities. Therefore, Table 6 outlines the set of selected normalized earthquakes along with their detailing and Fig. 9 will show the clear effect of the comparison of input data with design target spectra.

The normalization of the natural ground motion data set is the way to avoid unwarranted variability. Here, 30 ground motions data have been normalized by multiplying the factor calculated concerning PGA. Scaling of each ground motion is carried out by a scale factor according to Ansari and Agarwal (2016) and Vamvatsikos and Cornell (2002). A set of normalized earthquake data records to be collectively scaled upward or downward and the range of this scale factor depends on the failure of more than 50% damage of the structure (ATC and FEMA 2009). Approximately, 300 numerical analysis has been done for taking the output of all required IM and for each specified year.

Two different ground motion IM are used for plotting the IDA curves. These are the peak ground acceleration

Table 6 Properties of selected ground motions.

Earthquake number	Location of record	CAV values (g-s)	Strong duration (s)
EQ.1	Andong	3.78	8.52
EQ.2	Buyeo	7.10	32.09
EQ.3	Yeongcheon	4.20	11.12
EQ.4	Chilgok-gun	2.50	6.89
EQ.5	Ulsan	5.21	10.33
EQ.6	Donghae	2.71	3.96
EQ.7	Yeoju-gun	4.44	8.23
EQ.8	Geoje-si	6.55	19.95
EQ.9	Yeoncheon-gun	10.91	22.21
EQ.10	Sangju-si	4.35	9.01
EQ.11	Jinan-gun	4.71	23.53
EQ.12	Geoje-si	5.87	20.45
EQ.13	Byeonsan	2.37	19.58
EQ.14	Boryeong	3.02	18.96
EQ.15	Chungju	1.51	11.92
EQ.16	Daegok	2.63	12.84
EQ.17	Daegu	1.09	7.1
EQ.18	Gwangdong	0.82	4.32
EQ.19	Gumibo	2.36	11.49
EQ.20	Gampo	0.63	3.03
EQ.21	Gunwi	1.84	12.32
EQ.22	Hapcheon	2.11	16.06
EQ.23	Changnyeong	2.06	15.46
EQ.24	Hoengseong	1.01	4.19
EQ.25	Imha	1.52	8.13
EQ.26	Miryang	2.35	9.97
EQ.27	Namgang	1.42	5.58
EQ.28	Gangwon-do	1.64	8.52
EQ.29	Pyeongrim	1.74	11.75
EQ.30	Saengsong	1.54	13.13



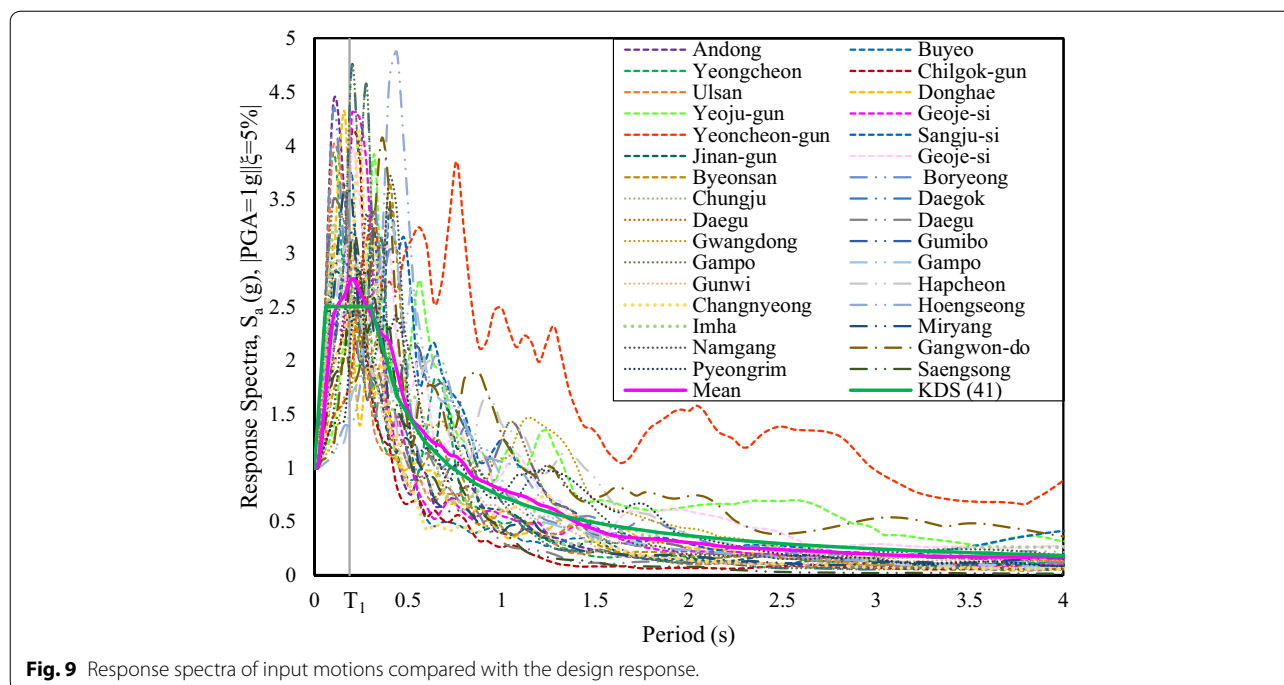


Fig. 9 Response spectra of input motions compared with the design response.

(PGA) and spectral acceleration at the structure’s first mode period (S_a).

3.7 Limit States Determination

Construction of fragilities for potential failure can be solved by observing the more severe limit states (Ellingwood and Tekie 2001) as mentioned above Sect. 2.3.1. Among several modes of failure criteria, two vulnerable points were taken to select the limit states for the seismic performance of this study. By analyzing the seismic result of the FEM, it was observed that the LS1 could be the neck or at the foundation zone. Even though the tensile stress is less than the compression, it may cause the crack of the dam body, which will be a significant issue that happens by investigating the relatively elastic and plastic strains on that zone. Therefore, from the parametric study in Tekie and Ellingwood (2003) and the result analysis, LS1 denotes the tensile damage at the foundation (heel of the dam) zone. The non-linear CDP consideration was captured in the cracking propagation in the dam body, where Fig. 4b presents the tensile softening behaviour of the taken CGD for the case study. The tensile damage follows the cracking length and the maximum tensile stress shows the first crack propagated identification. This is denoted as the splinting strength of concrete f_{sp} .

Note that, for showing the time-dependent seismic performance, each specific year was adopted for calculating

LS1, which will change according to the Eq. (11) (Mirza et al. 1979), because the splitting strength of concrete f_{sp} is correlated with the material modulus of elasticity (E). The time-dependent change in modulus of elasticity and corresponding splitting strength (LS1) of concrete is listed in Table 7.

The splitting strength is reduced with time as the modulus of elasticity is also reduced by the chemo-mechanical effect of concrete.

In the case of other limit states to get the threshold value of IM, the relative displacement on top of the dam with respect to heel is introduced here as LS2. The LS2 was taken for this dam 1.6 cm (0.028% of the monolith height of the dam), which had been remained constant throughout the seismic analysis of this study.

Table 7 Change of splitting strength of concrete (limit values for LS1).

Time, t (years)	Damaged concrete modulus of elasticity, E_e (MPa)	Splitting strength of concrete, f_{sp} (MPa)
0	13,269	1.49
10	12,611	1.42
20	11,667	1.31
30	11,164	1.25
40	10,649	1.19
50	10,146	1.14

4 Risk Assessment and Analysis of Aged CGD

4.1 Time-Dependent Fragility Analysis

To assess the chemo-mechanical effect on seismic vulnerability, the fragilities are estimated at different time points for the service life of the CGD. Figure 10 show the seismic performance for 0, 10, 20, 30, 40, and 50 years of the Bohyeonsan dam in terms of peak ground acceleration (PGA) and elastic pseudo-spectral acceleration (Sa), respectively. From Fig. 10a, it can be seen that for an example, the probability of tensile damage in the dam body is about 31% for an earthquake with a PGA of 1 g. Figure 10b shows the spectral acceleration approximately 4 g for the same percentage (31%) of failure probability in case of tension damage. These values are noticed for the zero years as well. The fragilities for LS2 are delineated corresponding to relative deformations of 1.6 cm (calculated as 0.028% of the monolith height) (Sen 2018; Tekie and Ellingwood 2003).

Figure 11 presents the ageing effect by the fragility performance with the HCLPF (Reed and Kennedy 1994) point for each specified year. The result shows a significant amount of change in IM for HCLPF points in the next 50 years. The PGA even Sa looks more critical for 5% failure probability in LS1 than LS2, where the main cause remains on the non-linear material property (NLMP) for

analysis. Even though this study shows the seismic fragility analysis using the 30 selected earthquakes in Korea, but it can be updated with different ground motions for other CGDs. In that case, the procedure described in the whole manuscript should be followed in the same way.

4.2 CAV Capacity of Aged CGD

To determine the CAV capacity for the aged CGD, all earthquake data sets (taken in this paper) are scaled with the smallest HCLPF PGA (Cao et al. 2019). The estimation of the CAV is to calculate the unscaled ground motion dataset by the threshold PGA. However, this PGA value is observed from Fig. 11a, where it presents a full form of failure probability of up to 50 years. The HCLPF PGA for two limits states is observed as like $LS1 < LS2$, and these are $0.27\text{ g} < 0.3\text{ g}$, $0.26\text{ g} < 0.29\text{ g}$, $0.23\text{ g} < 0.26\text{ g}$, $0.21\text{ g} < 0.23\text{ g}$, $0.19\text{ g} < 0.21\text{ g}$ and $0.17\text{ g} < 0.19\text{ g}$ for 0 year, 10 years, 20 years, 30 years, 40 years and 50 years, respectively. In each year for Bohyeonsan CGD, the tensile strength failure state gives the smallest PGA with comparing the relative displacement failure state. Therefore, for calculating the CAV, this smallest PGA gives safety measurement for the structure.

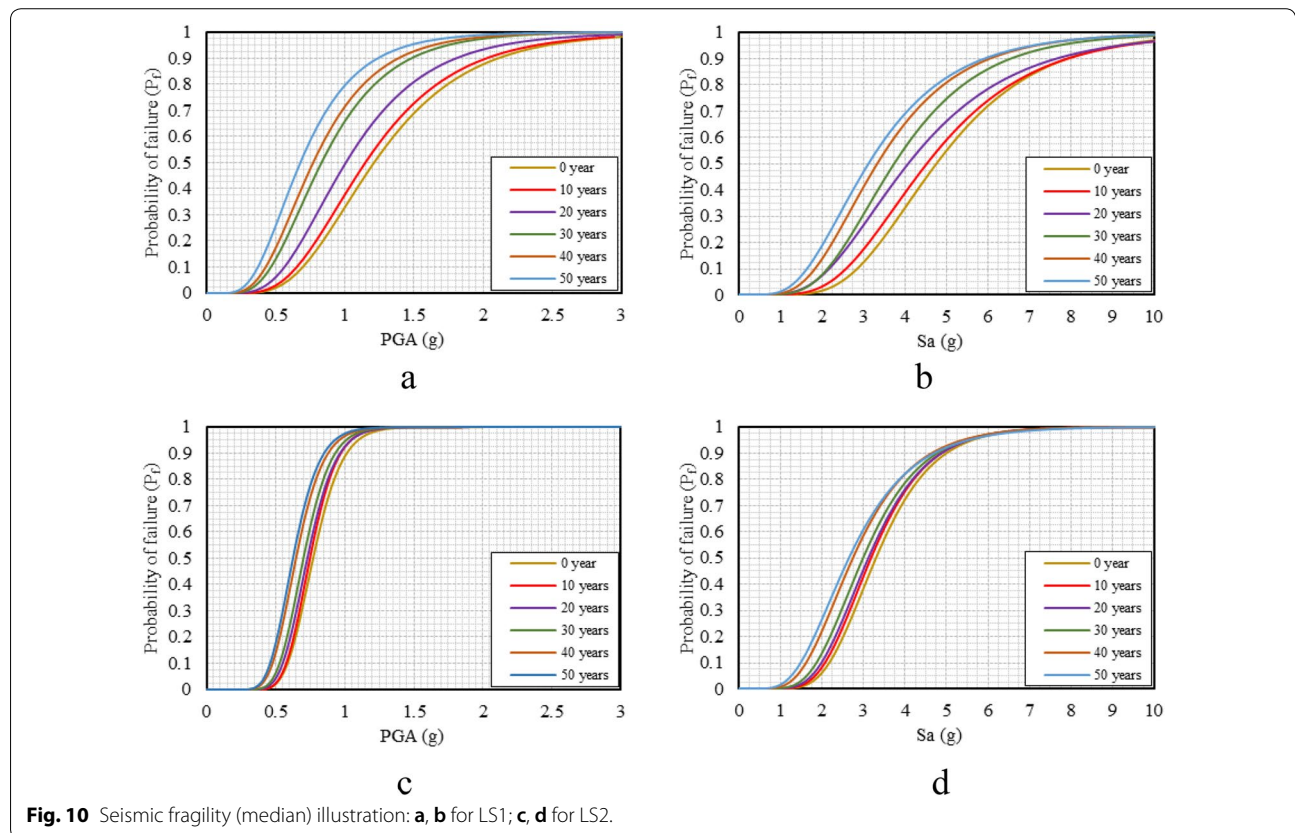


Fig. 10 Seismic fragility (median) illustration: **a, b** for LS1; **c, d** for LS2.

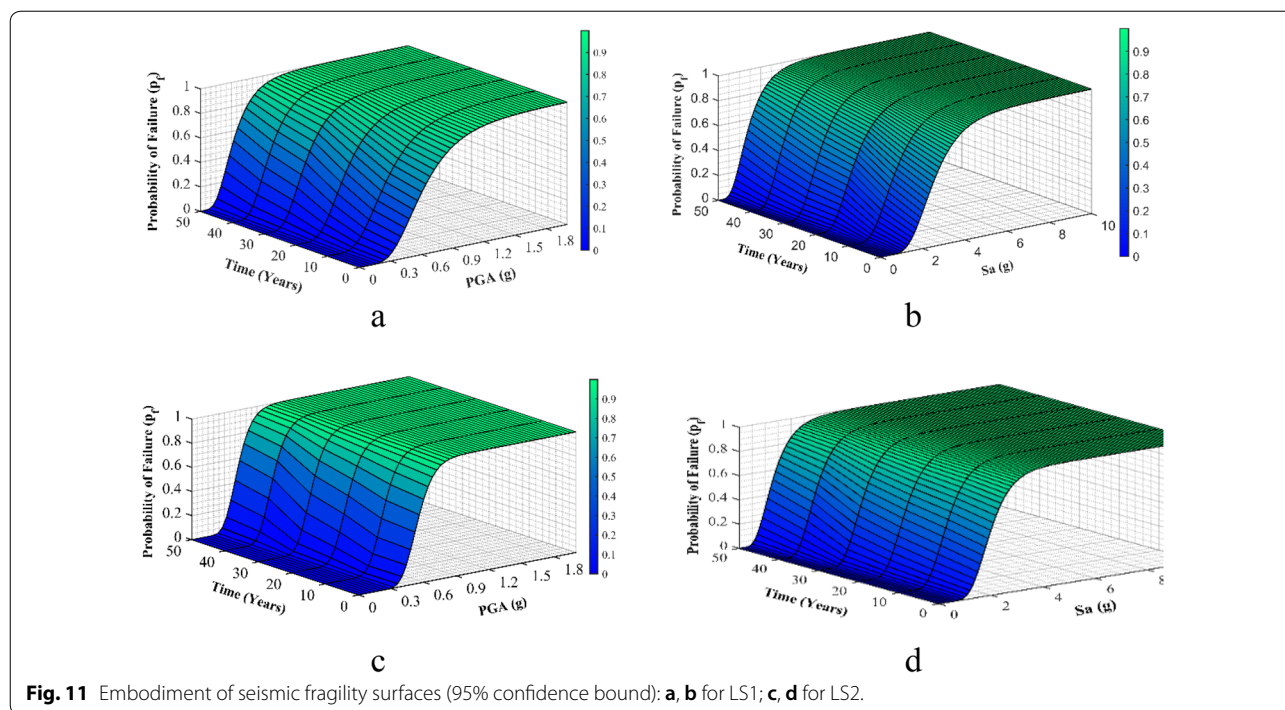


Fig. 11 Embodiment of seismic fragility surfaces (95% confidence bound): **a, b** for LS1; **c, d** for LS2.

In the previous study, the estimation of CAV directly from the fragility analysis of structure in terms of CAV (Mazilgüney et al.), which will give the most conservative result to quantify the seismic risk of the dam. Here, for each year, the capacity CAV has been calculated as the mean CAV value from selected earthquakes data sets. Table 8 is presenting the variation of CAV value with the time of 30 earthquake data sets.

Using the value in Table 8, Fig. 12 shows the three-dimensional normal distribution and linear regression analysis to give a model for CAV_{limit} capacity of Bohyeonsan CGD for each specified year. The model comes from the linear regression (LR) analysis depends on the time (years), where this time has a relation with the degradable young’s modulus of elasticity (E_c) and the model is expressed by the following equation:

$$CAV_{limit}(t) = -0.0057t + 0.5827. \tag{25}$$

This LR model has a minimum error of R^2 is 98%, which is acceptable fitting of the normal distribution. Using this capacity model, the result is gradually decreased with time, wherein the given entire time the capacity of CAV_{limit} value will vary from 0.61 to 0.36 g-s for 0 years to 50 years that is decreased by up to 40% from the present condition. As a result, the engineer or CGD operator can use this equation to predict the condition of structure at any time as well as assess the seismic risk of the degradable concrete gravity dams.

5 Conclusion

This research gives an approach to assessing and predicting the CGD capacity after some years by analyzing the failure probability with respect to the different limit states. The main concerning issue for a CGD is the material property when subjected to the time-dependent damage propagation. However, a time-dependent concrete-damaged plasticity model has been considered here for reflecting the chemo-mechanical effect of the concrete structure. To take the output reasonably, the water pressure was added using the Westergaard added mass method, and the numerical model was optimized by the RSM method. Previous studies were taken to compare with the modal analysis for proper validation and verification of FEM. However, the results can be explained as below:

1. The result from the optimized FEM shows the present material property of existing CGD (here Bohyeonsan CGD). After considering the ageing effect, the concrete modulus of elasticity has been decreased with time (here taken a maximum 50 years design period).
2. Using 30 selected ground motions in Korea, the time-variant seismic risk assessment has been done with the assistance of fragility function and CAV. The effect of degradation with time was carried out by the fragility analysis from the structural response using two different limit states (LS1 and LS2) in terms of

Table 8 Variation of CAV value with time (for LS1).

Earthquake number	Time, <i>t</i> (years)					
	0	10	20	30	40	50
EQ.1	0.560	0.540	0.480	0.400	0.350	0.330
EQ.2	0.590	0.580	0.510	0.420	0.380	0.350
EQ.3	0.690	0.670	0.590	0.490	0.440	0.410
EQ.4	0.400	0.390	0.340	0.280	0.250	0.240
EQ.5	0.530	0.510	0.450	0.370	0.330	0.310
EQ.6	0.280	0.270	0.240	0.200	0.180	0.170
EQ.7	0.540	0.520	0.460	0.380	0.340	0.320
EQ.8	0.910	0.880	0.780	0.640	0.570	0.540
EQ.9	1.130	1.090	0.960	0.790	0.710	0.670
EQ.10	0.410	0.390	0.350	0.290	0.260	0.240
EQ.11	0.400	0.390	0.340	0.280	0.250	0.240
EQ.12	0.400	0.390	0.340	0.280	0.250	0.240
EQ.13	0.620	0.580	0.490	0.350	0.320	0.290
EQ.14	0.527	0.490	0.400	0.320	0.290	0.260
EQ.15	0.511	0.460	0.380	0.310	0.270	0.250
EQ.16	0.353	0.320	0.250	0.210	0.190	0.180
EQ.17	0.378	0.350	0.290	0.230	0.200	0.180
EQ.18	0.340	0.310	0.270	0.220	0.190	0.170
EQ.19	0.656	0.600	0.550	0.450	0.350	0.300
EQ.20	0.810	0.750	0.690	0.610	0.450	0.380
EQ.21	0.698	0.640	0.570	0.490	0.390	0.340
EQ.22	0.777	0.750	0.650	0.570	0.470	0.440
EQ.23	0.894	0.810	0.750	0.660	0.550	0.480
EQ.24	0.571	0.520	0.450	0.390	0.310	0.280
EQ.25	0.529	0.490	0.390	0.310	0.290	0.250
EQ.26	0.655	0.620	0.550	0.480	0.430	0.380
EQ.27	0.743	0.710	0.620	0.540	0.490	0.410
EQ.28	0.255	0.210	0.190	0.170	0.160	0.150
EQ.29	0.327	0.300	0.250	0.210	0.190	0.170
EQ.30	0.761	0.740	0.690	0.550	0.480	0.420
Mean	0.575	0.542	0.476	0.396	0.344	0.313
Standard deviation	0.208	0.201	0.185	0.158	0.133	0.121

different intensity measures. The 5% failure probability is observed from the analysis of median value for LS1, which shows more vulnerability than LS2.

- The main reason behind more threshold value of PGA with increasing time is the tensile damage, which is directly related to the concrete strength. But, the change of relative displacement depends on the other issues.
- The fragility surface plot presents the three-dimensional illustration along with the HCLPF point of the structural response. From the HCLPF point, CAV is calculated for each specified year to predict CAV_{limit} capacity of degradable aged CGD. Because of reducing the energy content of the structure, CAV also

shows the same manner as compared to the fragility in different intensity measures.

- A capacity model is extracted from this research, where CAV_{limit} is a function of time (year). The assessment and prediction methods presented here are very effective, because of their time-saving and cost-effectiveness aspects.
- By following this approach, the operational inspection work can be checked at any time (year) and the probable damage can be figured out by the CAV_{limit} capacity of CGDs.
- Based on these, the engineers or CGD operators can get early warning action or can prevent the further failures of the structural components and accord-

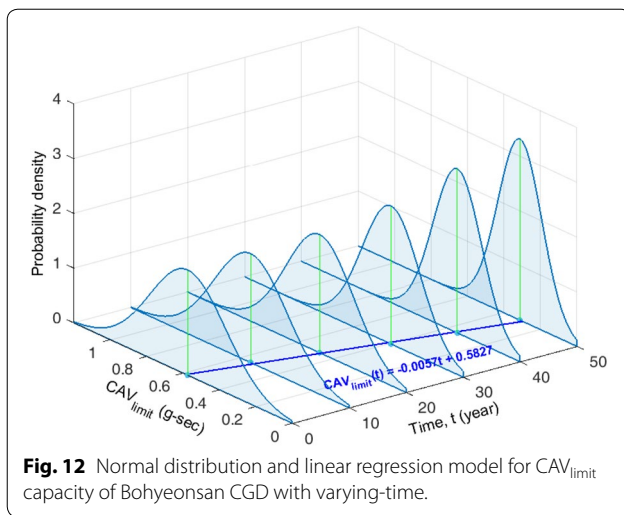


Fig. 12 Normal distribution and linear regression model for CAV_{limit} capacity of Bohyeonsan CGD with varying-time.

ing to the waring, they can get necessary steps to improve the accuracy and structural reliability.

The research can be extended to consider other parametric changes in concrete material property due to the ageing effect along with considering the fluid–foundation–dam interaction (FFDI).

Acknowledgements

Not applicable.

Authors' contributions

All authors have contributed to work and write the paper. All authors read and approved the final manuscript.

Authors' information

Ms. Tahmina Tasnim Nahar is currently doing her Ph.D. program in the Department of Civil & Environmental Engineering at Kunsan National University, Gunsan, Republic of Korea. Her research work is related to the RC structural health monitoring and retrofitting considering the different practical condition. She has also the 9 years teaching experience in RC structures as she is holding a teaching position in the Civil Engineering Department of Pabna University of Science and Technology, Bangladesh.

Mr. Anh-Tuan Cao is the graduated Master student from the Department of Civil & Environmental Engineering at Kunsan National University, Gunsan, Republic of Korea. His research work is focused on mainly RC structural health monitoring.

Prof. Dookie Kim is currently working as a Professor in the Department of Civil & Environmental Engineering, Kongju National University, Cheonan, Republic of Korea. His research field is related to structural engineering, dynamics, design and analysis, structural health monitoring, repairing and retrofitting, specialized analysis (Concrete), etc. He has published more than 400 papers in international journals and he has published 2 books.

Funding

This research was supported by a Grant (2017-MOIS31-002) from Fundamental Technology Development Program for Extreme Disaster Response funded by Korean Ministry of Interior and Safety (MOIS).

Availability of data and materials

Not applicable.

Competing interests

The authors declared that they have no competing interests.

Author details

¹ Department of Civil & Environmental Engineering, Kunsan National University, 558 Daehak-ro, Gunsan-si, Jeollabuk-do (Miryong-dong) 54150, Republic of Korea. ² Department of Civil & Environmental Engineering, Kongju National University, 1223-24 Cheonan-daero, Seobuk-gu, Cheonan, Chungcheongnam-do 31080, Republic of Korea.

Received: 30 January 2020 Accepted: 5 August 2020

Published online: 15 October 2020

References

- Alembagheri, M., & Ghaemian, M. (2013). Seismic assessment of concrete gravity dams using capacity estimation and damage indexes. *Earthquake Engineering and Structural Dynamics*, 42(1), 123–144. <https://doi.org/10.1002/eqe.2196>.
- Al-Shadeedi, M. B., & Hamdi, E. J. (2017). Stability evaluation of small concrete gravity dams. *Journal of Engineering and Sustainable Development*, 21(5), 15–38.
- Ansari, M. I., & Agarwal, P. (2016). Categorization of damage index of concrete gravity dam for the health monitoring after earthquake. *Journal of Earthquake Engineering*, 20(8), 1222–1238. <https://doi.org/10.1080/13632469.2016.1138167>.
- Ansari, M. I., Saqib, M., & Agarwal, P. (2018). Geometric configuration effects on nonlinear seismic behavior of concrete gravity dam. *Journal of Earthquake and Tsunami*, 12(01), 1850003. <https://doi.org/10.1142/S1793431118500033>.
- ATC, & FEMA. (2009). *Quantification of building seismic performance factors*. Federal Emergency Management Agency FEMA P695.
- Baker, J. W. (2015). Efficient analytical fragility function fitting using dynamic structural analysis. *Earthquake Spectra*, 31(1), 579–599. <https://doi.org/10.1193/021113EQS025M>.
- Bangert, F., Grasberger, S., Kuhl, D., & Meschke, G. (2003). Environmentally induced deterioration of concrete: Physical motivation and numerical modeling. *Engineering Fracture Mechanics*, 70(7–8), 891–910. [https://doi.org/10.1016/S0013-7944\(02\)00156-X](https://doi.org/10.1016/S0013-7944(02)00156-X).
- Bangert, F., Kuhl, D., & Meschke, G. (2001). Finite element simulation of chemo-mechanical damage under cyclic loading conditions. *Fracture Mechanics of Concrete Structures*, 1, 145–152.
- Birtel, V., & Mark, P. (2006). Parameterised finite element modelling of RC beam shear failure. In *ABAQUS users' conference* (pp. 95–108), Boston, USA.
- Brincker, R., Zhang, L., & Andersen, P. (2000, February 7–10). Modal identification from ambient responses using frequency domain decomposition. In *Proc. of the 18th international modal analysis conference (IMAC)* (pp. 625–630). Texas, USA.
- Campbell, K. W., & Bozorgnia, Y. (2012). Cumulative absolute velocity (CAV) and seismic intensity based on the peer-nga database. *Earthquake Spectra*, 28(2), 457–485. <https://doi.org/10.1193/1.4000012>.
- Cao, A.-T., Nahar, T. T., Kim, D., & Choi, B. (2019). Earthquake risk assessment of concrete gravity dam by cumulative absolute velocity and response surface methodology. *Earthquakes and Structures*, 17(5), 511–519. <https://doi.org/10.12989/eas.2019.17.5.511>.
- Champiri, M. D., Mousavi, M. M. R., Willam, K. J., & Gencturk, B. (2018). Effect of alkali-silica reactivity damage to tip-over impact performance of dry cask storage structures. *International Journal of Concrete Structures and Materials*, 12(1), 28. <https://doi.org/10.1186/s40069-018-0248-5>.
- Chopra, A. K. (2011). *Dynamics of structures: Theory and applications to earthquake engineering*. Upper Saddle River: Prentice Hall.
- Cornelissen, H., Hordijk, D., & Reinhardt, H. (1986). Experimental determination of crack softening characteristics of normalweight and lightweight. *Heron*, 31(2), 45–46.
- Dong, Y., Frangopol, D. M., & Saydam, D. (2013). Time-variant sustainability assessment of seismically vulnerable bridges subjected to multiple hazards. *Earthquake Engineering and Structural Dynamics*, 42(10), 1451–1467. <https://doi.org/10.1002/eqe.2281>.
- Du, W., & Wang, G. (2013). A simple ground-motion prediction model for cumulative absolute velocity and model validation. *Earthquake*

- Engineering and Structural Dynamics*, 42(8), 1189–1202. <https://doi.org/10.1002/eqe.2266>.
- Ellingwood, B., & Tekie, P. B. (2001). Fragility analysis of concrete gravity dams. *Journal of infrastructure systems*, 7(2), 41–48. [https://doi.org/10.1061/\(ASCE\)1076-0342\(2001\)7:2\(41\)](https://doi.org/10.1061/(ASCE)1076-0342(2001)7:2(41)).
- Fenfes, G. L., & Chopra, A. K. (1986). *Simplified analysis for earthquake resistant design of concrete gravity dams*. California: Ucbieerc-85/10, University of California, Earthquake Engineering Research Center.
- Ghosh, J., & Padgett, J. E. (2010). Aging considerations in the development of time-dependent seismic fragility curves. *Journal of Structural Engineering*, 136(12), 1497–1511. [https://doi.org/10.1061/\(ASCE\)ST.1943-541X.0000260](https://doi.org/10.1061/(ASCE)ST.1943-541X.0000260).
- Ghrib, F., & Tinawi, R. (1995). An application of damage mechanics for seismic analysis of concrete gravity dams. *Earthquake Engineering and Structural Dynamics*, 24(2), 157–173. <https://doi.org/10.1002/eqe.4290240203>.
- Gogoi, I., & Maity, D. (2007). Influence of sediment layers on dynamic behavior of aged concrete dams. *Journal of Engineering Mechanics*, 133(4), 400–413. [https://doi.org/10.1061/\(ASCE\)0733-9399\(2007\)133:4\(400\)](https://doi.org/10.1061/(ASCE)0733-9399(2007)133:4(400)).
- Grigoli, F., Cesca, S., Rinaldi, A. P., Manconi, A., Lopez-Comino, J. A., Clinton, J. F., et al. (2018). The November 2017 mw 5.5 pohang earthquake: A possible case of induced seismicity in South Korea. *Science*, 360(6392), 1003–1006. <https://doi.org/10.1126/science.aat2010>.
- Hardy, G., Merz, K., Abrahamson, N., & Watson-Lamprey, J. (2006). *Program on technology innovation: Use of cumulative absolute velocity (cav) in determining effects of small magnitude earthquakes on seismic hazard analyses*. EPRI report MD. 1014099, EPRI, Palo Alto, CA, and the US Department of Energy, Germantown.
- Hartford, D. N. D., & Baecher, G. B. (2004). *Risk and uncertainty in dam safety*. Heron Quay: Thomas Telford Publishing.
- Heo, Y., & Kunnath, S. K. (2013). Damage-based seismic performance evaluation of reinforced concrete frames. *International Journal of Concrete Structures and Materials*, 7(3), 175–182. <https://doi.org/10.1007/s40069-013-0046-z>.
- Ibarra, L. F., & Krawinkler, H. (2005). *Global collapse of frame structures under seismic excitations*, PEER Report 2005/06. Stanford: John A. Blume Earthquake Engineering Center P. E. E. R. Center.
- KCSC. (2016). *Korean design standard. 댐 설계 계획* (Design criteria for the Dam). KDS 54 10 15.
- KCSC. (2019). *Korean design standard. 건축물 내진설계기준* (Code for seismic design of buildings). KDS 41 17 00.
- Kim, J. H., Choi, I.-K., & Park, J.-H. (2011). Uncertainty analysis of system fragility for seismic safety evaluation of npp. *Nuclear Engineering and Design*, 241(7), 2570–2579. <https://doi.org/10.1016/j.nucengdes.2011.04.031>.
- Ko, S., Cho, S. G., Kim, D., & Cui, J. (2009). Modal identification of cabinets of nuclear power plant based on experimental study. *대한토목학회 학술대회*, 826–829.
- Kuhl, D., Bangert, F., & Meschke, G. (2004a). Coupled chemo-mechanical deterioration of cementitious materials part ii: Numerical methods and simulations. *International Journal of Solids and Structures*, 41(1), 41–67. <https://doi.org/10.1016/j.ijsolstr.2003.08.004>.
- Kuhl, D., Bangert, F., & Meschke, G. (2004b). Coupled chemo-mechanical deterioration of cementitious materials. Part i: Modeling. *International Journal of Solids and Structures*, 41(1), 15–40. <https://doi.org/10.1016/j.ijsolstr.2003.08.005>.
- Lupoi, A., & Callari, C. (2011). The role of probabilistic methods in evaluating the seismic risk of concrete dams. In M. Dolšek (Ed.), *Protection of built environment against earthquakes* (pp. 309–329). Berlin: Springer. https://doi.org/10.1007/978-94-007-1448-9_15.
- Manandhar2b, S., & Cho, H.-I. (2018). New site classification system and design response spectra in korean seismic code. <https://doi.org/10.12989/eas.2018.15.1.001>.
- Mandal, T. K., Ghosh, S., & Pujari, N. N. (2016). Seismic fragility analysis of a typical indian phwr containment: Comparison of fragility models. *Structural Safety*, 58, 11–19. <https://doi.org/10.1016/j.strusafe.2015.08.003>.
- Mandal, K. K., & Maity, D. (2015). Influence of hygro-chemo-mechanical degradation on performance of concrete gravity dam. *World Academy of Science, Engineering and Technology, International Journal of Civil, Environmental, Structural, Construction and Architectural Engineering*, 9(2), 199–204. <https://doi.org/10.5281/zenodo.1107467>.
- Mazilgüney, L., Yakut, A., Kadaş, K., & Kalem, İ. (2013). Fragility analysis of reinforced concrete school buildings using alternative intensity measure-based ground motion sets. In *2nd Turkish conference on earthquake engineering and seismology* (pp. 25–27) Hatay, Türkiye.
- Mirza, S. A., MacGregor, J. G., & Hatzinikolas, M. (1979). Statistical descriptions of strength of concrete. *Journal of the Structural Division*, 105(6), 1021–1037.
- Mridha, S., & Maity, D. (2014). Experimental investigation on nonlinear dynamic response of concrete gravity dam-reservoir system. *Engineering Structures*, 80, 289–297. <https://doi.org/10.1016/j.engstruct.2014.09.017>.
- Myers, R. H., Montgomery, D. C., & Anderson-Cook, C. M. (1995). *Response surface methodology: Process and product optimization using designed experiments*. Hoboken: Wiley.
- Nakamura, H., Nanri, T., Miura, T., & Roy, S. (2018). Experimental investigation of compressive strength and compressive fracture energy of longitudinally cracked concrete. *Cement & Concrete Composites*, 93, 1–18. <https://doi.org/10.1016/j.cemconcomp.2018.06.015>.
- Nayak, P., & Maity, D. (2013). Seismic damage analysis of aged concrete gravity dams. *International Journal for Computational Methods in Engineering Science and Mechanics*, 14(5), 424–439. <https://doi.org/10.1080/15502287.2013.784380>.
- Nguyen, D. V., Kim, D., Park, C., & Choi, B. (2019). Seismic soil–structure interaction analysis of concrete gravity dam using perfectly matched discrete layers with analytical wavelengths. *Journal of Earthquake Engineering*. <https://doi.org/10.1080/13632469.2019.1595222>.
- Nie, J., Braverman, J., Hofmayer, C., Choun, Y. S., Kim, M. K., & Choi, I. K. (2010). *Fragility analysis methodology for degraded structures and passive components in nuclear power plants illustrated using a condensate storage tank*, KAERI/TR-4068/2010; BNL-93771-2010, Korea Atomic Energy Research Institute.
- O'Hara, T. F., & Jacobson, J. P. (1991). *Standardization of the cumulative absolute velocity*, EPRI-TR-100082, Electric Power Research Inst. & Yankee Atomic Electric Co.
- Pakzad, S. (2018). *Dynamics of civil structures, volume 2: Proceedings of the 36th imac, a conference and exposition on structural dynamics 2018*. Springer.
- Pan, J., Zhang, C., Wang, J., & Xu, Y. (2009). Seismic damage–cracking analysis of arch dams using different earthquake input mechanisms. *Science in China Series E: Technological Sciences*, 52(2), 518–529. <https://doi.org/10.1007/s11431-008-0303-6>.
- Prassinios, P. G., Ravindra, M., & Savy, J. B. (1986). *Recommendations to the nuclear regulatory commission on trial guidelines for seismic margin reviews of nuclear power plants: Draft report for comment*. NUREG/CR-4482, UCID-20579, Lawrence Livermore National Lab.
- Reed, J., & Kennedy, R. (1994). *Methodology for developing seismic fragilities epr tr-103959*. Palo Alto: Electric Power Research Institute.
- Sadhukhan, B., Mondal, N. K., & Chattoraj, S. (2016). Optimisation using central composite design (ccd) and the desirability function for sorption of methylene blue from aqueous solution onto lemna major. *Karala International Journal of Modern Science*, 2(3), 145–155. <https://doi.org/10.1016/j.kijoms.2016.03.005>.
- Sen, U. (2018). *Risk assessment of concrete gravity dams under earthquake loads*. Master's Thesis, Louisiana State University Louisiana, USA. Retrieved from https://digitalcommons.lsu.edu/gradschool_theses/4730/.
- Shah, C. (2002). Mesh discretization error and criteria for accuracy of finite element solutions. In *Ansys users conference*.
- Tekie, P. B., & Ellingwood, B. R. (2003). Seismic fragility assessment of concrete gravity dams. *Earthquake Engineering and Structural Dynamics*, 32(14), 2221–2240. <https://doi.org/10.1002/eqe.325>.
- Vamvatsikos, D., & Cornell, C. A. (2002). Incremental dynamic analysis. *Earthquake Engineering and Structural Dynamics*, 31(3), 491–514. <https://doi.org/10.1002/eqe.141>.
- Wahalathantri, B. L., Thambiratnam, D., Chan, T., & Fawzia, S. (2011). A material model for flexural crack simulation in reinforced concrete elements using abaqus. In *Proceedings of the first international conference on engineering, designing and developing the built environment for sustainable wellbeing* (pp. 260–264).
- Wan, K., Li, Y., & Sun, W. (2012). Application of tomography for solid calcium distributions in calcium leaching cement paste. *Construction and Building Materials*, 36, 913–917. <https://doi.org/10.1016/j.conbuildmat.2012.06.069>.

- Wang, J., Jin, F., & Zhang, C. (2011). Seismic safety of arch dams with aging effects. *Science China Technological Sciences*, 54(3), 522–530. <https://doi.org/10.1007/s11431-010-4279-7>.
- Wang, J., Yun, X., Kuo-Chen, H., & Wu, Y.-M. (2018). CAV site-effect assessment: A case study of taipei basin. *Soil Dynamics and Earthquake Engineering*, 108, 142–149. <https://doi.org/10.1016/j.soildyn.2018.02.028>.
- Washa, G. W., Saemann, J. C., & Cramer, S. M. (1989). Fifty-year properties of concrete made in 1937. *Materials Journal*, 86(4), 367–371.

- Westergaard, H. M. (1933). Water pressures on dams during earthquakes. *Transaction of ASCE*, 95, 418–433.

Publisher's Note

Springer Nature remains neutral with regard to jurisdictional claims in published maps and institutional affiliations.

Submit your manuscript to a SpringerOpen[®] journal and benefit from:

- ▶ Convenient online submission
- ▶ Rigorous peer review
- ▶ Open access: articles freely available online
- ▶ High visibility within the field
- ▶ Retaining the copyright to your article

Submit your next manuscript at ▶ [springeropen.com](https://www.springeropen.com)
